Positron annihilation in low-temperature rare gases. I. Helium

K. F. Canter,* J. D. McNutt,† and L. O. Roellig
Department of Physics, Wayne State University, Detroit, Michigan 48202
(Received 24 June 1974; revised manuscript received 19 May 1975)

The lifetime spectra of positrons annihilating in helium gas have been obtained over the temperature range 4.6-300 K and the density range 0.016-0.030 g/cm^3. The spectra are decomposed into slow-positron and ortho-positronium annihilation components which are presented and discussed separately. At low temperatures, the density and temperature dependences of the data are found to depart markedly from the usual behavior observed at room temperature. Simple quantitative treatments are given of the cluster model for the slow-positron data and of the cavity model for the ortho-positronium results.

I. INTRODUCTION

When a positron is emitted at high energies into helium-4 gas, there are many processes by which it can arrive at its eventual annihilation with one of the helium atomic electrons. By discriminating against the time at which the annihilation occurs after emission, it is often possible to analyze the various processes separately. In particular, the processes of most interest are the annihilations of slow positrons and of positrons which form ortho-positronium (o-Ps) prior to annihilation. Early experiments[1,2] have shown that at very low temperatures o-Ps and slow-positron annihilation differ significantly from the comparatively simple free-particle annihilation properties observed in helium gas at higher temperatures.[3] The purpose of the experiments described in this article is to shed light on the low-temperature phenomena by observing the effect of changing gas temperature as well as density on the lifetime spectra of o-Ps and slow positrons, with particular emphasis on the latter, in gaseous helium. Immediately following this article, another paper describes subsequent variable temperature experiments in neon and argon gas which were carried out to see what conclusions drawn from the helium results could be related to the annihilation of positrons in other rare gases.

The distinction between slow-positron and o-Ps annihilation processes can best be visualized by briefly describing the way in which positrons approach thermalization after being emitted into the gas. First, the positrons rapidly undergo several thousand inelastic collisions until they are scattered into the energy region below 19.8 eV, the excitation energy for the first excited state of the helium atom.[4] Below this energy, the positrons can either undergo elastic collisions with the gas atoms or remove an atomic electron and form the electron-positron atom, positronium. The latter process is only possible if the positron's energy is above 17.7 eV, the ionization energy of helium minus the binding energy of o-Ps. Due to the large number of small-energy-loss elastic collisions required for a positron to lose an electron volt or so of energy, most of the positrons which are initially scattered into the region 19.8 to 17.7 eV form positronium rather than slow down out of this region via elastic collisions with the gas atoms. On the other hand, the positrons that have been inelastically scattered into the region below the positronium formation threshold 17.7 eV can only undergo elastic collisions and are hereafter referred to as slow positrons. Of the positrons which form positronium, one-fourth form the short-lived spin singlet state para-positronium (p-Ps) and the remaining three-fourths form the spin triplet state o-Ps which suffers a much slower rate of annihilation.

Since the process by which the positrons form o-Ps or become slow positrons is irreversible (when no externally applied electric fields are present), we can regard the two groups of positrons as two distinct species. Following a description in Sec. II of this paper of the experimental procedure employed, slow positrons and o-Ps are treated separately in Secs. III and IV, respectively. Section V summarizes the picture of positron annihilation in general for gaseous helium.

II. EXPERIMENTAL PROCEDURE

A. Cryogenics and gas handling

Figure 1 shows the details of the helium-gas sample chamber and the tail section of the variable temperature cryostat used for most of the reported measurements. The positron source inside the sample chamber consisted of 2 μCi of ^{22}Na deposited on a thin Mylar film, which was then sealed inside a hollow aluminum needle of 1.5 mm diameter and 0.07 mm wall thickness. The fraction of positrons which stopped in the

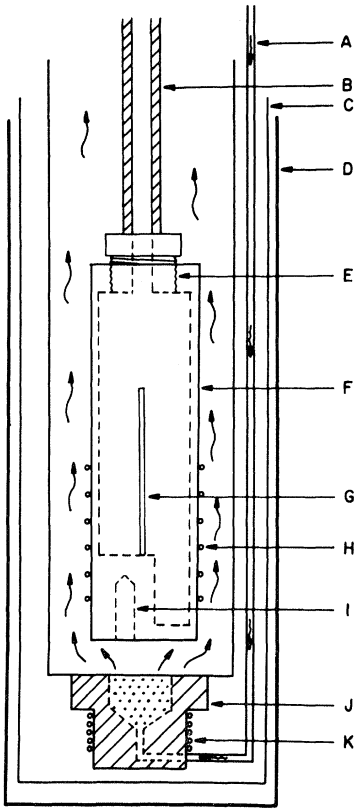

FIG. 1. Gas sample chamber and tail section of variable temperature cryostat: (A) Capillary which supplies cryogen from cryogen Dewar above the tail section, (B) vacuum-insulated sample-gas supply tube, (C) heat shield, (D) outer wall of tail section, 4.8 cm diameter, (E) pipethread seal, pretinned with Woods metal, (F) sample chamber, 7.6 cm long, 1.9-cm inside diameter, and 0.16-cm wall thickness, (G) hollow aluminum needle with ^{22}Na source inside, (H) heater coil, (I) thermometry, (J) porous plug which vaporizes cryogen, (K) heater coil.

sample gas varied from 10 to 25%, depending on the density being investigated. This represented an improvement of nearly a factor of 3 over the stopping fraction obtained using a conventional foil sandwich as the source container and moderating assembly.

The variable temperature cooling of the sample chamber was achieved by flowing vaporized liquid helium around the outer walls of the chamber. This cooling was in turn balanced by heater coils which could control the temperature of the cooling vapor and the sample chamber directly. In practice, the rate of vapor flow and the heating current supplied to the vaporizing block were manually set at a constant level such that no more than 30 mW of additional heat needed to be supplied to the heater coil on the sample chamber. The current to the latter coil was supplied by the output of a power supply having both proportional reset as well as rate action feedback features. The control unit was able to maintain a temperature stability of 0.05% throughout the duration of a three-day run. The thermometry for the control system consisted of manufacturer calibrated germanium[5] and platinum[6] resistance thermometers. The germanium resistor was used to cover the range 4–28 K, and the platinum resistor covered the range 20–300 K. Numerous checks for consistency of temperature readings with vapor pressure as well as pressure-vs-temperature measurements on the sample gas were carried out in our laboratory to make sure that the thermometry calibration conformed to the accuracy quoted by the manufacturers. In this way we were able to place upper limits of 0.4 and 0.2% on the absolute and relative errors, respectively, for the measured values of the gas temperature.

Equally important as the temperature accuracy is the question of spatial uniformity of temperature across the dimensions of the gas sample chamber. Because of rotational symmetry, we need only consider a possible temperature gradient along the length of the sample chamber. If, in the worst possible case, the heating and cooling were localized at opposite ends of the chamber, then the resulting temperature gradient would correspond to a heat flow along the walls of the chamber equal to the rate of heat supplied to balance the cooling. Taking into account the thermal conductivity of the copper sample chamber[7] and the amount of heater current used, a temperature differential across the length of the chamber of less than 0.5% of the average temperature was calculated for all temperatures investigated. Additional checks on the temperature accuracy and uniformity were provided by comparisons of the data obtained from the variable temperature experiments and a series of fixed temperature runs at 5.0 K and at various gas densities. The latter experiments were carried out by submersing the sample chamber directly into the liquid-helium cryogen in a conventional helium Dewar. The cryogen was then pressurized to a pressure of 1.94 atm absolute in order to achieve a temperature of 5.0 K. Comparisons between the variable and fixed temperature experiments will be discussed further in Sec. III.

The sample gas pressure was measured to an accuracy of 99% or better using several Bourdon-tube gauges on the gas supply system with overlapping pressure scales throughout the range 1–150 atm. The gas densities were then calculated from analytical fits to experimental thermodynamic data.[8] Combining the errors due to pressure and temperature readings and to using ana-

lytical fits yielded an estimate of 1% as the upper limit on the absolute error in calculated gas densities for temperatures above 8 K. For the temperature range 4–8 K the absolute and relative errors in gas density were estimated to be 4 and 2%, respectively.

The helium-gas composition, as quoted by the supplier,[9] consisted of the following impurities (in ppm): N_2, 2.8; O_2, 0.7; Ne, 11.8; and H_2O, 1.8. The remaining impurities were below the minimum detectable limits of 0.1 ppm. A sequence of evacuating, filling, and venting the system was repeated many times to guarantee that no additional atmospheric impurities were introduced into the gas. It is not as easy, however, to assess the degree to which impurities related to the intrinsic cleanliness of the gas supply system were removed. The system, which was constructed of stainless-steel tubing (6.34 mm diameter) and solderless fillings, was cleaned with high-purity trichloroethylene before assembly and then evacuated to mechanical pump pressures for an accumulative period of several weeks. At temperatures less than 10 K or so, any impurities would condense out as very-low-vapor-pressure solids and hence be of no concern. Aside from the precautions taken in handling the gas, we also relied on comparing certain features of the data at room temperature with the data below 10 K as a confirmation of the gas purity at higher temperatures.

B. Lifetime measuring electronics

The emission of a positron into the gas by the ^{22}Na source is accompanied by the essentially simultaneous emission of a 1.28-MeV γ ray. The subsequent annihilation of the positron yields two or three γ rays, each of which is 0.51 MeV or less in energy. The photomultiplier (PM) assemblies consisted of 3.5 × 3.5 cm Naton-136 plastic scintillators optically coupled to Amperex 1021 PM tubes. The PM anode pulses resulting from the detection of the 1.28 MeV and an annihilation γ ray were fed directly into the start and stop inputs, respectively, of an Ortec 437 time-to-amplitude converter (TAC). The TAC output, which is directly proportional to the time difference between the start and stop input signals, was then fed into a 256-channel multichannel analyzer (MCA). The PM dynode pulses were used for γ-ray energy identification and subsequent gating of the TAC output pulses into the MCA. Prompt, i.e., simultaneous, emission and annihilation events were simulated using a ^{60}Co γ source. The full width at half-maximum of the prompt-resolution spectrum was 1.2 nsec. The time calibration of the TAC was obtained by measuring the effect of delaying the stop input pulses with calibrated delay lines on the location of centroid of the prompt-resolution spectrum recorded in the MCA. Differential linearity curves of the TAC were also taken as a check on the time calibration. The maximum deviation of the time calibration from a linear fit to the time-versus-TAC output (as recorded in the MCA) was found to be 1.8%. The constant of proportionality in the time-versus-channel number fit could be determined from the delay-line measurements to within an error of less than 0.5%.

C. Data analysis

The stored data in the MCA is printed out as a record of the number of annihilations versus the time interval between emission and annihilation of the positrons. The plotted record, which is referred to as a time decay or lifetime spectrum, can also represent the annihilation activity $A(t)$ that would result if all the positrons were hypothetically introduced into the gas at the same time ($t = 0$). The distinction between the hypothetical ensemble or "swarm" of positrons and the actual case of the positrons, for the most part, being emitted one at a time by a low activity (2 μCi) source will not be made in further sections of this paper.

Each lifetime spectrum is decomposed into the sum of the following components: prompt annihilations, background random coincidences, o-Ps annihilations, and the annihilation of slow positrons. The prompt component, which arises from the rapid annihilation of positrons that are not stopped in the gas sample and from the annihilation of para-positronium, usually cannot be accurately subtracted from the spectra, but vanishes within a short time (<5 nsec) after $t = 0$. For this reason, we usually ignore this portion of the lifetime spectra. The background component for $t > 0$ is taken as a time-independent constant which is proportional to the average background that is visible in the $t < 0$ region of the spectra. The constant of proportionality differed from unity by only a few percent and was linearly interpolated as a function of gas density from values which were directly measured when spectra were taken in vacuum and at high gas densities. The error bars shown for the o-Ps and slow-positron lifetimes include the estimated error incurred in the background subtraction as well as the calculated statistical error which was found to be the larger of the two sources of error.

The o-Ps component was separated from the slow-positron component by applying a least-squares-weighted fit to two exponentials[10] from

time t_e onwards, where t_e is the time after which the slow positrons can be regarded as annihilating via exponential decay. An incorrect choice of t_e so that the decay is not truly exponential (i.e., the slow positrons have not reached equilibrium) from t_e onwards would produce a systematic error in the analysis. It was found that the slow-positron equilibrium decay rate λ_e obtained from the fitting program would increase as t_e was increased until any further increase in t_e resulted in no further change, within statistical errors, in λ_e. Hence, t_e was always chosen in such a way that any systematic error in λ_e associated with its choice was comparable to or less than the statistical error quoted for λ_e. The o-Ps component, however, was assumed to be exponential for $t < t_e$ as well as for $t > t_e$ and was subtracted accordingly from the spectra.

III. SLOW POSITRONS

A. Experimental data

A total lifetime spectrum of positrons annihilating in helium gas at a temperature of 5.50 K and a density of 0.023 g/cm^3 (=129 amagat) is shown in Fig. 2. The slow annihilation components observed at two different temperatures, but at the same gas density, are shown in detail in Fig. 3. The 5.50-K spectrum is characterized by a slightly nonexponential shoulder having a weak bump [B], followed by a peak, which is ultimately followed by a region of exponential decay with an associated equilibrium decay rate λ_e. At the higher temperature of 7.50 K, the spectrum exhibits the same weak bump observed in the low-temperature spectrum, but no peak is present. Spectra taken at higher temperatures up to room temperature were found to be identical, within errors, to the 7.50 K spectrum. Figure 4 illustrates the way in which the low-temperature spectra take on the appearance of the high-temperature spectra as the temperature is increased with gas density held constant. At each of the three densities investigated, we can assign a value of temperature T_H, above which a further increase in temperature has no visible effect on the spectra. The values of T_H are roughly 5.3, 6.5, and 8.0 K corresponding to the densities 0.016, 0.023, and 0.030 g/cm^3, respectively. The spectra taken at temperatures greater than T_H are referred to as high-temperature spectra, as opposed to the low-temperature spectra for $T < T_H$. As T approaches T_H from below, the peak in the low-temperature spectra occurs at later times and, in addition, becomes weaker until it is lost in the statistical fluctuations of the recorded counts (annihilations). The temperature dependence of λ_e

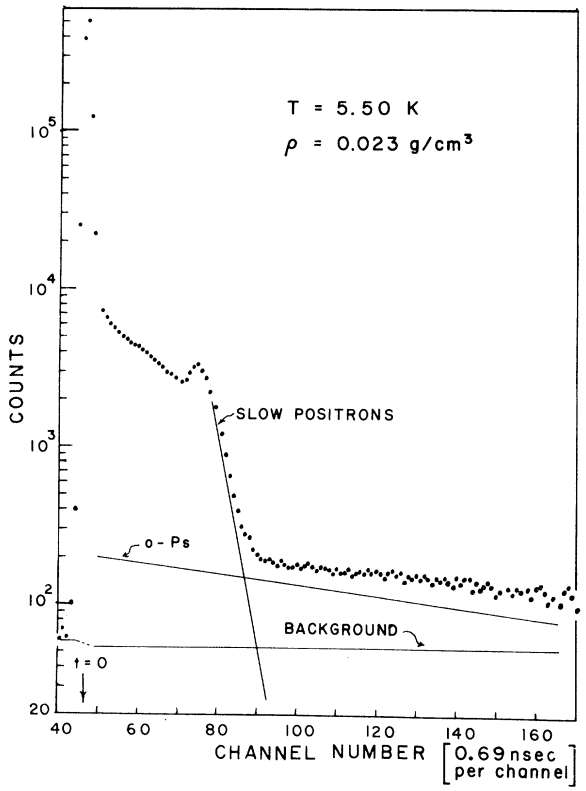

FIG. 2. Total lifetime spectrum showing the separation of o-Ps and background components.

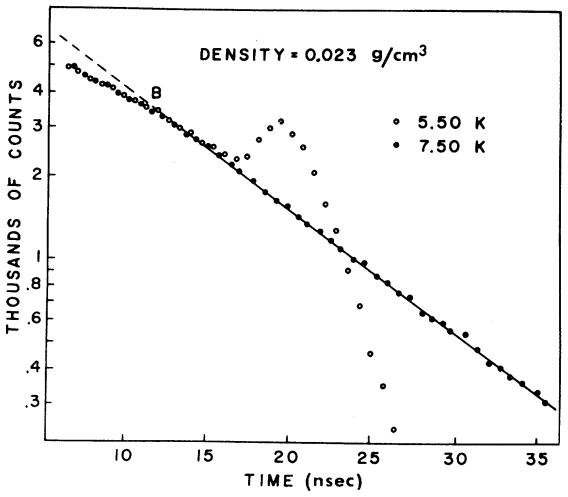

FIG. 3. Two slow-positron annihilation components with equal normalization at 5.50 and 7.50 K. The dashed-line extrapolation of the exponential decay fit to the 7.5 K emphasizes the nonexponential shoulder region common to both spectra.

obtained from the variable-temperature cryostat experiments is shown in Fig. 5. The lowest temperature investigated at each density was chosen so as to avoid the appropriate condensation temperature by at least 0.05 K. The density dependence of λ_e is explicitly demonstrated in Fig. 6 where the values shown were obtained from the fixed-temperature cryostat experiments. The agreement between values of λ_e obtained from the two types of experiments is very good at the same values of densities and temperatures. This is especially important for the value of λ_e measured at 5.00 K and 0.016 g/cm^3. As shown in Figs. 5 and 6, λ_e is very sensitive to density and temperature in this region. In view of the radically different methods of cooling and measuring temperature in the fixed- and variable-temperature experiments, this agreement is a reassuring check on the reproducibility of the low-temperature effects.

B. Discussion

It has been shown by Leung and Paul that the features of the high-temperature spectra can

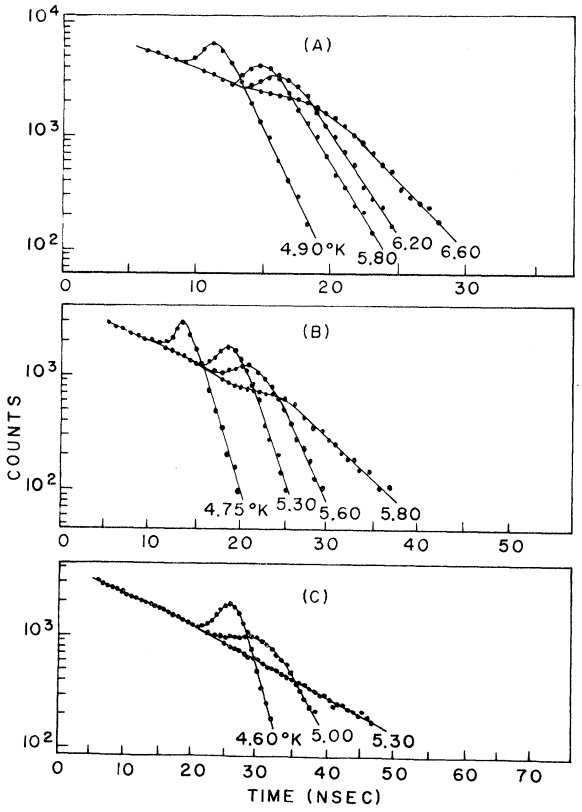

FIG. 4. Slow-positron spectra at the densities (A) 0.030, (B) 0.023, and (C) 0.016 g/cm^3. In order to identify the spectra at each temperature, a curve is drawn through the set of points corresponding to the given gas temperature.

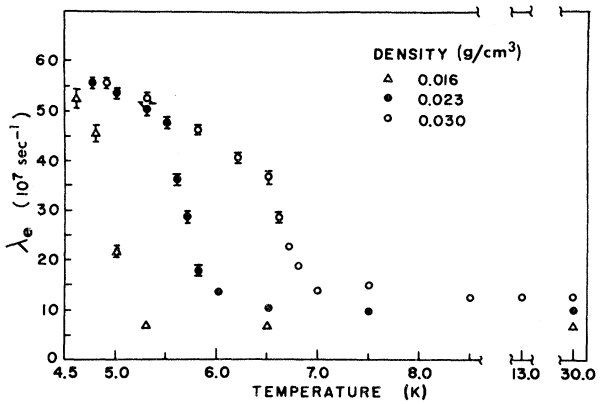

FIG. 5. Equilibrium decay rates of slow positrons in helium gas. Error bars have been omitted when they fall within the size of the plotted points.

quantitatively be accounted for in terms of the classical diffusion picture of positrons slowing down towards thermal equilibrium via elastic collisions with the gas atoms.[3] The agreement between theory and experiment, however, is dependent on knowing the scattering and annihilation cross sections for positron-helium collisions. Although these cross sections are not precisely known at present, there is enough evidence to believe that Drachman's cross sections, as used by Leung and Paul to describe their data, provide at least a qualitatively accurate picture of the annihilation and elastic scattering of free positrons in helium. Briefly, the weak bump in the spectra (observed at [B] in Fig. 3) is attributed to a 20% increase in $Z(\mathcal{E})$, which is equivalent to the annihilation probability per collision, as the positron energy E decreases from approximately 1 eV down

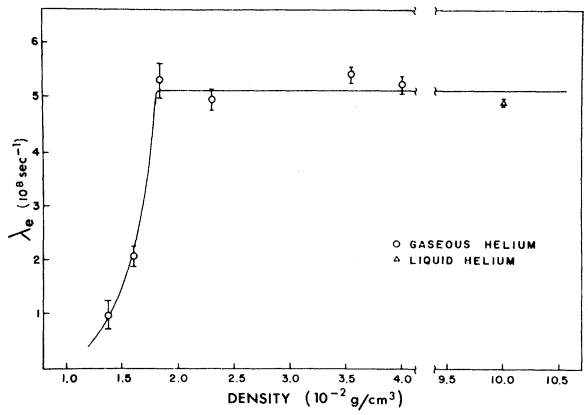

FIG. 6. Equilibrium decay rate of slow positrons as a function of density with temperature constant at 5.0 K. The highest density point taken in the gas phase corresponds to saturated helium vapor with a small amount of condensed helium in the bottom of the sample chamber.

to thermal energies. The reason that the bump is well localized is that the positrons slow down through this region in a comparatively short time because the scattering cross section undergoes a large increase in this energy region as well. The location of the weak bump is also referred to as the "shoulder width" t_s and is inversely proportional to the gas density. Within errors, there was no detectable difference between the shoulder widths (multiplied by gas density) measured in the low-temperature and high-temperature spectra. The value of t_s obtained by eye for each spectrum was found to fall within the range $\rho t_s = 1150 \pm 150$ nsec amagat, where ρ is the gas density in units of amagats (1 amagat $= 1.78 \times 10^{-4}$ g/cm^3 for helium-4).

At low temperatures, after the positrons have slowed down through the energy region associated with the weak bump, there is a much more severe increase in $Z(E)$ when the positrons reach a lower energy which we denote as E_R. Tao and Kelly[11] have been able to produce good fits to the original low-temperature spectra of Roellig and Kelly[1] by solving the appropriate diffusion equations with the inclusion of a sudden increase in $Z(E < E_R)$ of up to a factor of 6.5 greater than Drachman's values at low energies. The location of the resulting peak in the calculated spectrum is then determined by the particular choice of E_R and the momentum-transfer cross section $\sigma(E)$.

We can obtain an approximation of the relation between the choice of E_R needed to fit the spectra and the particular choice of $\sigma(E)$ by assuming that the location of the peak is the time required to slow down from $E_0 = 17.7$ eV to E_R with an average rate of energy loss given by

$$\frac{dE}{dt} = \frac{2}{M}(2mE)^{1/2}(E - 2kT)n\sigma(E), \tag{1}$$

where m and M are the positron and helium atom masses, respectively, and n is the number density.[12] If we then use $\sigma(E)$ as adopted by Leung and Paul, it is found that E_R must be less than 0.01 eV and decrease slightly ($\approx 2 \times 10^{-3}$ eV/K) with respect to an increase in temperature in order to account for the location of the peak in each spectrum.[13] It is also found that other choices of $\sigma(E)$, which are consistent with Drachman's estimates and not at drastic variance with Leung and Paul's choice, can be made such that the position of the peak in each spectrum can be accounted for with a single value of E_R, $(1.3 \pm 0.1) \times 10^{-3}$ eV. In such a situation, the shift in the peak with increasing temperature is then simply a result of the fact that it takes longer for the positrons to slow down to a given energy, via elastic collisions, when the gas atoms are moving faster. However, it must be emphasized that Eq. (1) gives the average rate of decrease of positron energy, rather than the rate of decrease of the average positron energy. The latter quantity would give a more realistic relation between E_R and the location of the peak, but requires considerably more computational effort than the simplified slowing-down equations. Whether or not E_R is independent of temperature should be considered an open question until the role of temperature in full diffusion calculations, similar to those of Tao and Kelly, has been fully investigated.

In addition to the kinematical considerations involved in trying to account for the location of the peak, the unusual temperature and density dependence of the equilibrium decay rate might be considered as a separate phenomenon in itself. Not only can λ_e be extremely sensitive to changes in temperature and density, but also the decay rate departs drastically from the direct proportionality to gas density expected for free positrons. Also, as shown in Fig. 6, the low-temperature decay rate of positrons in helium gas can become as large as the value observed in bulk helium *liquid*. It was this feature of the early low-temperature spectra that prompted Roellig's suggestion[14] that at low temperature the positron becomes surrounded by a cluster of condensed helium, which is similar to the electrostricted cluster proposed by Atkins for positive ions in liquid helium.[15]

The simplest treatment of the positron-induced cluster is to assume that the helium is a continuum and is electrostricted about a localized positron having a spherically symmetric wave function. Denoting the helium density as $n(r)$ at a distance r from the cluster center, the resulting annihilation rate can be expressed as

$$\lambda_e = \pi r_0^2 c Z_0 \int_0^\infty u^2(r) n(r)\, dr, \tag{2}$$

where $u(r) = (4\pi)^{1/2} r \Psi(r)$ is the equivalent one-dimensional positron wave function and Z_0 is taken to be 3.9, the value for which Eq. (2) yields the observed high-temperature decay rates for free positrons when $u(r)$ is a plane wave. Here, r_0 is the classical electron radius and c is the velocity of light. In order to calculate $n(r)$, the electrostatic force of attraction due to the positron's electric field $\epsilon(r)$ on a volume element of the helium cluster is equated to the repulsive force arising from the resulting hydrostatic pressure gradient, i.e.,

$$\alpha n(r) \epsilon(r) \frac{d\epsilon(r)}{dr} = \frac{dP(r)}{dr}, \tag{3}$$

where $P(r)$ is the fluid pressure at r and α is the helium atomic polarizability. Integrating (3) from

r to infinity, setting $n(\infty)$ equal to the bulk density n_0 and $\epsilon(\infty)$ equal to zero yields

$$\int_{n_0}^{n(r)} \left(\frac{\partial P}{\partial n}\right)\frac{dn}{n} = \tfrac{1}{2}\alpha\,\epsilon^2(r). \tag{4}$$

The above equation was originally derived by Atkins, using a thermodynamic approach.[15] The electric field produced by the positron is given by the Gauss law as

$$\epsilon(r) = \frac{q\int_0^r u^2(r')dr'}{r^2[1+4\pi\alpha n(r)]}, \tag{5}$$

where q is the positron charge, in cgs units.

As a first guess for obtaining $u(r)$, we solve the Schrödinger equation for a positron localized by the potential well $V(r)$ given by

$$V(r) = -4\pi q\alpha \int_r^\infty \frac{\epsilon(r')n(r')\,dr'}{1-\frac{4}{3}\pi\alpha n(r')}, \tag{6}$$

which in turn depends on $u(r)$.

It is found that regardless of the initial choice for $u(r)$, the resulting $V(r)$ does not allow a bound-state solution to the Schrödinger equation. This prevents obtaining a self-consistent solution, aside from the trivial solution of $u(r)$ becoming infinite in extent, i.e., a free particle. It is therefore concluded that the induced polarization attraction between the positron and helium as a polarizable fluid is insufficient by itself to hold the cluster together. Since induced polarization is an overestimate of the actual attraction between a positron and a helium atom,[16] this conclusion should also be valid in the face of a more realistic treatment of the interaction between the positron and the individual helium atoms. However, if the problem were treated realistically in its entirety, multiple scattering of the positron wave function by the helium atoms, as well as possible chemical bonds between the positron and a few atoms in the cluster, might aid in producing a stable cluster.

It is of interest to note that if we increase the positron mass in the Schrödinger equation (as a means of taking into account possible mechanisms in addition to induced polarization which serve to localize the positron) to six times its actual mass, that a self-consistent bound-state solution to the above equations can be found. In such a case the solutions converge to a "hyperbound" solution with the positron localized within a region of about 1 Å in diameter, surrounded by a solid core of helium atoms, and having a decay rate of approximately 10^9 sec^{-1} (nearly twice the maximum observed decay rate). However for a positron localized within a region of atomic dimensions, we have to abandon treating the gas as a continuum. In spite of this shortcoming, the calculated decay rates can be made to simulate the observed "critical" sensitivity of λ_e to small changes in T and n_0 by making a suitable choice of the initial trial solution. This is because there are two extremes for stable solutions, the hyperbound and unbound solutions,[17] and which of the two the solutions converge to is critically dependent in T and n_0.

Even if we accept that the above treatment of the cluster model qualitatively accounts for the effect of temperature and density on the equilibrium decay rates, we are still faced with having to postulate the existence of a mechanism which takes a free positron from its unlocalized state into a state which is localized enough as to allow the gas atoms to respond to the positron's electric field. It would not be difficult to find many features of the positron-helium problem that could lead to departures from the free-positron picture. A list of possibilities might include positron–single-helium-atom bound states,[18] inhomogeneities in the intrinsic gas structure such as multiatom clusters,[19] and quantum-mechanical effects associated with the multiple scattering of the positron wave function.[20] Regardless of the possibility explored, however, it is difficult to imagine that all of the features of the low-temperature effects can be accounted for without also including the electrostrictive effects, as treated above, in the calculations.

IV. ORTHO-POSITRONIUM

A. Experimental data

Some representative values of the measured decay rates of o-Ps in helium are shown in Fig. 7. Although many more values were obtained at temperatures and densities other than those shown in the figure, most had to be discarded because of large errors associated with the poor statistics. This is partly due to the experimental method here being tailored to look mainly at the slow-positron component, i.e., fast timing resolution with attendant losses in counting efficiency. However, it was possible to obtain the low-temperature decay rates shown by taking data over extended periods of time. The room-temperature (300 K) data are considerably better because the sample chamber was removed from the cryostat, which allowed the photomultipliers to be placed closer to the sample chamber with a resulting fivefold increase in counting rate.

B. Discussion

The solid line in Fig. 7 was obtained from a least-squares-weighted linear fit to the four 300 K decay rates. The fit yielded a zero-density inter-

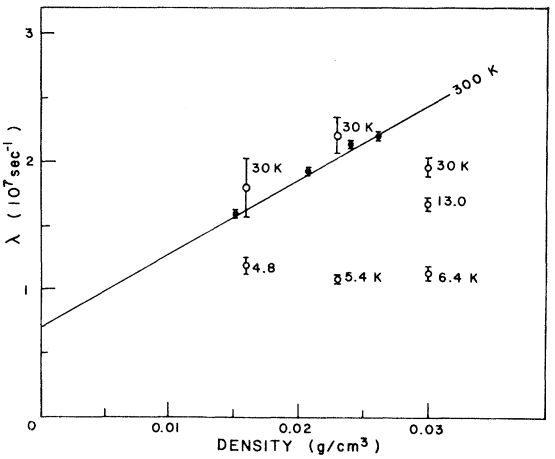

FIG. 7. Decay rates of o-Ps in helium gas. The solid circles were obtained at room temperature (300 K) with the photomultipliers close to the sample chamber.

cept of $(0.70\pm 0.14)\times 10^7$ sec^{-1}, which is in agreement with the known decay rate of o-Ps undergoing self-annihilation in vacuum $\lambda_{vac} = 0.72\times 10^7$ sec^{-1}. Because of this agreement and the linearity of λ vs ρ, we assume that the room-temperature decay rates are characteristic of free o-Ps in gases, i.e.,

$$\lambda_{free} = \lambda_{vac} + (4\pi r_0^2 c/M)\,{}^1Z_{eff}\rho\,, \tag{7}$$

where M is the helium-atom mass and ${}^1Z_{eff}$ is the number of electrons per gas atom, as seen in the singlet state relative to the positron spin of the o-Ps atom. To reduce the statistical error in determining ${}^1Z_{eff}$ from the room-temperature data, we reapplied a least-squares fit to the data with the constraint $\lambda = \lambda_{vac}$ at $\rho = 0$ The resulting value of ${}^1Z_{eff}$ was found to be 0.129 ± 0.006, the significance of which will be discussed momentarily.

The deviation of the low-temperature decay rates from the room-temperature values given by (7) is similar to the effects observed by Roellig and Kelly[2] Their data was applied to a model in which the increase in lifetime at lower temperatures is attributed to the o-Ps being trapped in a cavity in the gas. Likewise, such an interpretation is applicable here. Treating the o-Ps as a point particle, its decay rate is given by

$$\lambda = \lambda_{vac}(1 - P_{out}) + \lambda_{free} P_{out}\,, \tag{8}$$

where P_{out} is the fraction of the o-Ps probability density which extends beyond the cavity into the gas. Here it is assumed that the cavity has a well-defined radius R and is void of any helium atoms. Using (8), we can solve for P_{out} in terms of the observed low-temperature decay rate λ and the free o-Ps annihilation rate in the bulk gas λ_{free}, which is given by the fit to the room temperature, i.e., no cavity, decay rates. In this way, we can treat P_{out} as the measured quantity which is to be accounted for by the cavity model. As a result of the multiple scattering of the o-Ps wave function,[21] the helium gas outside the cavity presents a potential barrier to the o-Ps which is responsible for confining the o-Ps in the cavity. Assuming for the moment that a cavity of radius R can be represented by a spherical square well of depth V_0 and radius R, it is easy to show that P_{out} can be expressed as

$$P_{out} = \sin^2\eta/(1 - \eta\cot\eta)\,, \tag{9}$$

with

$$\eta/\sin\eta = (2mV_0/\hbar^2)^{1/2}R, \quad \tfrac{1}{2}\pi \leq \eta \leq \pi\,. \tag{10}$$

Thus, for a given choice of R and V_0, (10) is solved for η which is then substituted into (9) to calculate the corresponding P_{out}. The condition that η lie between $\frac{1}{2}\pi$ and π is a way of imposing the assumption that the potential well is shallow enough so as to allow only one bound state. We can proceed further by imposing the condition that the pressure exerted by the o-Ps, due to its nonzero ground-state kinetic energy E_z, be balanced by the gas pressure p outside the cavity, i.e.,

$$p = \frac{-1}{4\pi R^2}\frac{\partial E_z}{\partial R}\,, \tag{11}$$

where

$$E_z = V_0 \sin^2\eta\,. \tag{12}$$

Changing the variable of differentiation from R to η in (11) and using (12) along with (10) yields the following condition for a stable cavity:

$$V_0^{5/2} = 2\pi p\left(\frac{\hbar^2}{2m}\right)^{3/2}\frac{\eta^2(\eta\cot\eta - 1)}{\sin^4\eta\cos\eta}\,. \tag{13}$$

As cumbersome as the introduction of the variable η might appear, in practice it greatly reduces the amount of calculations needed to account for P_{out} in terms of V_0 at each pressure. The course of action is as follows: Plotting P_{out} vs η as given by (9), allows us to determine the particular value of η corresponding to each low-temperature decay rate and the associated free o-Ps decay rate. Inserting this value of η into (13) then yields V_0, where it is assumed that p can be taken as the measured bulk gas pressure. Thus, V_0 becomes the only variable parameter of the model. The values of V_0 corresponding to the measured decay rates are shown in Fig. 8. The corresponding cavity radii, calculated from (10), are also given. Figure 8 becomes particularly relevant when compared with the theoretical prediction made by the multiple scattering model[21]:

$$V_0 = (2\pi/m_p)na\hbar^2\,, \tag{14}$$

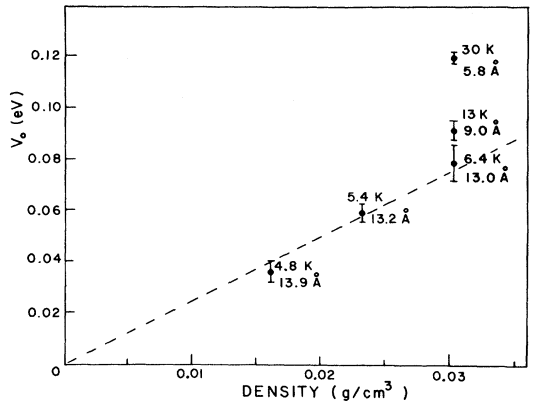

FIG. 8. Values of potential well depth necessary for cavity model to account for the observed o-Ps decay rates. The corresponding calculated equilibrium cavity radius R for each data point is given in Angstrom units next to each point. The dashed line is a least-square-weighted fit, constrained to pass through the origin, to the three largest cavity radius points.

where m_p is the mass of the particle in the cavity (i.e., $m_p = o$-Ps mass $= 2\times$electron mass) and a is the zero-energy scattering length for positronium-helium collisions.

Although the above expression for V_0 does not include the effects due to interactions between the helium atoms,[22] the necessary corrections for *gaseous* helium are not large enough to account for the differences in V_0 corresponding to the highest density points shown in Fig. 8. It is more likely that these points do not coincide because our simplified treatment of the cavity model becomes increasingly unreliable as the equilibrium cavity radius decreases at higher temperatures and associated pressures. Aside from the validity of the model as a function of cavity radius, the lower-temperature points are also easier to treat since the contribution of the radius-dependent entropy contributions to the total free energy of the cavity become neglible compared to $E_z + \frac{4}{3}\pi R^3 p$ as $T \to 0$. On the assumption that the larger radius (13–14 Å) cavities serve as realistic tests of the cavity model, a least-squares-weighted fit constrained to pass through the origin (dashed line in Fig. 8) was drawn through these points to best determine the proportionality constant of V_0 vs n, in accordance with (14). From this fit, the scattering length was found to be $a = 0.77 \pm 0.04$ Å, which is in good agreement with the recent value calculated by Drachman and Houston, 0.735 Å.[23] Further, their calculation yields ${}^1Z_{\text{eff}} = 0.098$ which is to be compared with the value, ${}^1Z_{\text{eff}} = 0.129 \pm 0.006$, used to obtain our "measured" value of the scattering length.

The reliability of the measured ${}^1Z_{\text{eff}}$ perhaps needs close examination before we can claim any degree of success in measuring the scattering length. Our value of ${}^1Z_{\text{eff}}$ is in agreement with Duff and Heyman's value 0.118 ± 0.016,[24] but disagrees markedly from the most recent value 0.180 ± 0.016 measured by Beers and Hughes.[25] The two largest sources of systematic errors in any of these measurements are improper background subtraction and the presence of atmospheric impurities, notably O_2 which is a good quencher of o-Ps.[26] A good indication of the accuracy of the background subtraction is the agreement between the zero-density extrapolated decay rate and λ_{vac}. The presence of impurities which remain a constant fraction of the helium density does not affect this agreement, but manifests itself in values of ${}^1Z_{\text{eff}}$ which are too large. These facts, in addition to our being able to produce a shoulder in the slow-positron spectrum indicate that ${}^1Z_{\text{eff}}$ is more likely to lie within the lower range (0.118 ± 0.011)–(0.129 ± 0.006) rather than be as large as the Beers and Hughes value.

Up until this point, our discussion of the cavity model has avoided direct mention of the closely related subjects of angular correlation measurements of para-positronium (p-Ps)[27] and electron mobility[22,28] experiments in fluid helium. The latter has been the subject of almost all of the theoretical treatments of the cavity model which, fortunately, are equally as applicable to describing the configuration of the cavity induced by a Ps atom as they are in the case of the electron-induced cavity. Analogous to the increase in lifetimes of o-Ps which becomes localized in a cavity, extraordinarily low mobilities of electrons of helium are accounted for by the motion of the electron along with its "bubble" under the influence of externally applied electric fields. The most important new development in the cavity model description of the electron mobilities has been the introduction of the "pseudobubble" model by Eggarter and Cohen.[29,30] This model has yielded the best agreement to date between the measured and calculated electron mobilities in the low-gas-density region ($\lesssim 10^{-2}$ g/cm^3) where the effects of gas-density fluctuations are large enough to require a departure from the simple picture of the gas as a homogeneous medium.[31] However at higher, near-saturated densities where the mobilities are very low, a self-consistent rounding off of the corners of the potential well associated with the cavity is sufficient for quantitatively accounting for these mobilities.[28] This modification is probably less important for our purposes since the lifetime of o-Ps is not very sensitive to the precise shape of the cavity. On the other hand, the consequences of using the pseudobubble model

may be large if we are in the density and temperature region where the "cavity" is far from being completely void of any helium atoms in its interior. Thus, further appraisal of the lifetime method of measuring the positronium-helium scattering length should be reserved until the Eggarter-Cohen theory is applied to our temperatures and densities along with the calculated potential well depths V_0.

With regard to cavities induced by p-Ps, angular correlation measurements of the $2\text{-}\gamma$ annihilation have unambiguously demonstrated positronium-induced cavity formation in liquid helium.[27] The distinction between p-Ps and o-Ps in cavities can be dropped, insofar as both of these principle ground states of Ps have the same scattering length for scattering with helium atoms.[32] The distinction can be removed entirely if the cavity can attain its "equilibrium" configuration within a time less than the lifetime of p-Ps, 1.25×10^{-10} sec, which is to be compared with the much longer lifetime of o-Ps, $\approx10^{-7}$ sec.[33] If it is possible to carry out a high-statistics angular correlation experiment, then it should also be possible to directly measure V_0 and R via the effect of these parameters on the momentum distribution of the p-Ps.

V. SUMMARY

At temperatures greater than approximately 10 K, the lifetime spectra of slow positrons annihilating in helium gas can be accounted for in terms of the scattering and annihilation cross sections for positron collisions with single helium atoms. The spectra at lower temperatures defy such a simple explanation. The positrons annihilate in the same manner as they do at higher temperatures as they approach thermal equilibrium until they reach some value of energy, whereupon the annihilation rate rapidly increases to an anomalously large value. The temperature and density dependence of this annihilation rate is reminiscent of the vapor-liquid phase transition and lends support to the hypothesis that the increase in annihilation rate is a result of the positrons becoming surrounded by a condensed cluster of electrostricted helium atoms. Further improvements in the cluster model as well as an evaluation of the mechanism responsible for the initiation of the cluster are necessary to obtain quantitative verification of the hypothesis. The theoretical picture for o-Ps induced cavities may be clearer, but more experimental data is needed for verification of the model.

ACKNOWLEDGMENTS

The authors would like to thank A. S. Deshpande for his assistance with the slowing-down calculations and for attending some of the runs. The many conversations with Professor L. D. Favro and Professor A. M. de Graaf concerning the cluster model were very helpful and are gratefully acknowledged.

---

*Present address: Department of Physics, Brandeis University, Waltham, Mass. 02154.

†Present address: Department of Physics, University of Texas at Arlington, Arlington, Tex. 76019.

[1]L. O. Roellig and T. M. Kelly, Phys. Rev. Lett. 15, 476 (1965).

[2]L. O. Roellig and T. M. Kelly, Phys. Rev. Lett. 18, 387 (1967).

[3]C. Y. Leung and D. A. L. Paul, J. Phys. B 2, 1278 (1969).

[4]S. J. Tao, J. H. Green, and G. J. Celitans, Proc. Phys. Soc. Lond. 81, 1091 (1963).

[5]Supplied by Andonian Associates Inc., Waltham, Mass. 02154.

[6]Supplied by Rosemount Engineering Co., Minneapolis, Minn. 54435.

[7]The sample chamber material was 99.9% pure (O_2 is the nominal impurity), electrolytic tough-pitch, "hard-drawn" copper bar stock having an average thermal conductivity of 4 W/cm K over the range 5–30 K. See R. L. Powel, H. M. Roder, and W. M. Rogers, J. Appl. Phys. 28, 1282 (1957).

[8]D. B. Mann, *Thermodynamic Properties of Helium*, U. S. Natl. Bur. Stand. Technical Note No. 154 (U. S. GPO., Washington, D. C., 1962).

[9]Matheson Inc., Gas Products Division, Joliet, Ill. 60434.

[10]S. J. Tao, IEEE Trans. Nucl. Sci. NS-15, 176 (1968).

[11]S. J. Tao and T. M. Kelly, Phys. Rev. 185, 135 (1969).

[12]S. J. Tao, J. H. Green, and G. J. Celitans, Proc. Phys. Soc. Lond. 81, 1091 (1963).

[13]There is a possibility that E_R is slightly density dependent as well, since the location of the peak was found not to be precisely inversely proportional to gas density at a given value of temperature. However, improved density determinations and a consistent criterion for specifying the location of the peak is necessary before the possibility of E_R being density dependent can be explored further.

[14]L. O. Roellig, *Positron Annihilation*, edited by A. T. Stewart and L. O. Roellig (Academic, New York, 1967), pp. 127–141.

[15]K. R. Atkins, Phys. Rev. 173, 190 (1968).

[16]H. S. W. Massey, J. Lawson, and D. G. Thompson, *Quantum Theory of Solids*, edited by P. Lowdin (Academic, New York, 1966), pp. 203–215.

[17]It was found possible to choose $u(r)$ in such a way that the first iterated solution can approximate $u(r)$ to any accuracy desired. However, this was an unstable self-consistent solution since successive iterations inevitably

departed from the trial solution and rapidly converged to either the unbound or hyperbound solution.
[18]At present there is no realistic theoretical treatment of the e^+-He system that predicts a stable bound state when the He atom is in its ground state. In fact, it is becoming a general consensus that such a bound state cannot exist. See F. H. Gerter, H. B. Snodgrass, and L. Spruch, Phys. Rev. 172, 110 (1965).
[19]D. E. Stogryn and J. O. Hirschfelder, J. Chem. Phys. 31, 1531 (1959).
[20]M. H. Coopersmith, Phys. Rev. A 4, 295 (1971).
[21]M. H. Coopersmith, Phys. Rev. 139, A1359 (1965).
[22]J. L. Levine and T. M. Sanders, Phys. Rev. 154, 138 (1967).
[23]R. J. Drachman and S. K. Houston, J. Phys. B 3, 1657 (1970).
[24]B. G. Duff and F. F. Heyman, Proc. Phys. Soc. Lond. A 270, 517 (1962).
[25]This value of Beers and Hughes is quoted by P. A. Fraser, J. Phys. B 1, 1006 (1969).
[26]G. J. Celitans, S. J. Tao, and J. H. Green, Proc. Phys. Soc. Lond. 83, 833 (1964).
[27]C. V. Briscoe, S. I. Choi, and A. T. Stewart, Phys. Rev. Lett. 20, 493 (1968).
[28]H. R. Harrison and B. E. Springett, Phys. Lett. 35A, 73 (1971). See also, J. P. Hernandes, Phys. Rev. A 5, 635 (1972).
[29]T. P. Eggarter and M. H. Cohen, Phys. Rev. Lett. 26, 129 (1971).
[30]T. P. Eggarter, Phys. Rev. A 5, 2496 (1972).
[31]A major difference between the pseudobubble and the simple bubble presented here is the degree of penetration of helium atoms into the interior of the cavity.
[32]R. J. Drachman (private communication).
[33]J. P. Hernandes and M. Silver, Phys. Rev. A 2, 1949 (1970).